

# Fuel consumption prediction of civil air crafts using deep learning: a comparative study

Quoc Hung Nguyen, Hoang Lan Nguyen

School of Business Information Technology, UEH College of Technology and Design, University of Economics Ho Chi Minh City (UEH), Vietnam

## Article Info

### Article history:

Received Jun 30, 2024

Revised Apr 21, 2025

Accepted May 10, 2025

### Keywords:

Aircraft trajectory prediction

Deep neural networks

Mutual information feature selection

Prediction of jet fuel consumption

Recurrent neural networks

## ABSTRACT

Accurate fuel consumption prediction is critical for minimizing the adverse impact of fuel emissions on the environment, conserving fuel, and reducing flight costs. Additionally, precise fuel forecasting enhances trajectory prediction and supports effective air traffic management. This study evaluates the predictive performance of two deep learning techniques in predicting the fuel consumption of a civil aircraft belonging to Airbus A320NEO. Based on the analysis, the findings show that the deep neural network (DNN) model has better score of indicators and than the recurrent neural network (RNN) including mean absolute error (MAE), mean squared error (MSE), root mean squared error (RMSE) and R-squared ( $R^2$ ). By integrating an automated feature selection approach with an optimized deep learning framework, this research contributes to the development of a robust and efficient predictive system for fuel consumption. The findings have practical implications for improving fuel management strategies in aviation, leading to cost savings and reduced emissions. One limitation of this study is its reliance on specific environmental variables, which may limit the model's generalizability across different flight conditions, aircraft types, and operational scenarios.

This is an open access article under the [CC BY-SA](#) license.



## Corresponding Author:

Quoc Hung Nguyen

School of Business Information Technology, UEH College of Technology and Design

University of Economics Ho Chi Minh City (UEH)

59C Nguyen Dinh Chieu Street, Xuan Hoa Ward, District 3, Ho Chi Minh City, Vietnam

Email: hungnq@ueh.edu.vn

## 1. INTRODUCTION

The aviation industry is a major contributor to global greenhouse gas emissions, primarily through its production of  $CO_2$ . In 2010, the international aviation industry consumed approximately 142 million tons of fuel, resulting in 448 million metric tons (Mt, 1 kg  $\times$  109) of emissions  $CO_2$ , and fuel consumption is expected to 2.8–2.9 times by 2040 [1]. However, by 2013, the total gas  $CO_2$  generated from commercial flights had reached 707 million tons and futher increase to 920 million tons by 2019 (about 30% in 6 years) [2], [3]. Aircraft engines produce  $CO_2$  as a fixed ratio of 3.16 kg  $CO_2$  per 1 kg of burned fuel, making it a persistent green house gas [4]. Its long lifetime in the atmosphere makes  $CO_2$  a potent greenhouse gas. Once emitted,  $CO_2$  remains in the atmosphere for centuries, with 20 percent remain for thousands of years [5]. Therefore, all the emissions generated from aircraft will take many time to be converted. The COVID-19 pandemic temporarily reduced global flight activity in 2020 by nearly 50%, significantly decreasing greenhouse gas emissions [6], [7]. This sharp decline underscores the aviation sector's profound environmental impact and highlights the urgent need for sustainable solutions. Furthermore, the continued growth in passenger numbers exacerbates the problem. In

2010, the industry transported 2.4 billion passengers, a figure projected to reach 8.2 billion by 2040 [8]–[10]. Thus, aviation-related emissions could triple by 2050 compared to 2015 levels [11], [12].

To mitigate these impacts, the European Union Commission has been applying solutions such as sustainable aviation fuels (SAF) and flight routes optimizations [13]. However, to apply solutions, current forecasting models for fuel consumption have many variations, leading to  $CO_2$  large deviations in the calculation of impacts and other emissions. Besides, poor predictions can result in financial losses for airlines by failing to detect aircraft malfunctions in time.

The contribution of paper is using deep learning model including deep neural network (DNN) and recurrent neural network (RNN) to predict accurately aircraft fuel consumption of a long distance. Flight monitors data is used for fueling consumption assessment. An underscored point in the paper is an optimized process using opened and efficient models, features selection method to easily put the model into practices. As a result, two main focused points in the paper are features selection method (mutual information (MI)) and the good deep learning model (the result of comparison between DNN and RNN). The involvement of big data, powerful tools are required to transform those data before running the process.

## 2. METHOD

### 2.1. Definition of quick access recorder data

A quick access recorder (QAR) [14] is a system that can easily and quickly collect aircraft data. It consists of an airborne device for data recording and a ground software station for data storage and analysis. QAR can capture approximately 2000 parameters per aircraft, including position, motion, operations, and warnings, but its data remains confidential and is rarely used in research [15]. Unlike flight data recorders (FDR) and cockpit voice recorders (CVR), QARs are not mandatory and are typically installed in easily accessible locations, such as airline cabins, for routine monitoring of aircraft systems and crew performance [16], [17]. QAR data is translated through a data decoding frame (also known as a dataframe). It receives input from the flight data acquisition unit and has evolved from using magnetic tapes to solid-state memory. Previously, data had to be manually retrieved, processed, and stored, leading to significant operational costs. However, modern wireless technology now allows secure, real-time transmission of compressed and encrypted QAR data via mobile networks, improving efficiency, reducing costs, and enhancing data availability [18].

### 2.2. Mutual information

Mutual information (MI) [19] quantifies the dependence between two random variables. A high MI [20] score indicates a strong relationship with the target variable, making it useful for prediction. A low MI score indicates suggests minimal influence, while an MI score of zero signifies complete independence [21]. For two discrete variables  $X$  and  $Y$  with a joint probability distribution of  $P_{XY}(x, y)$ , the value of MI of this distribution is denoted  $I(X; Y)$  with the following formula:

$$I(X; Y) = \sum_{xx}^X \sum_{yy}^Y P_{XY}(x, y) \log \frac{P_{XY}(x, y)}{P_X(x)P_Y(y)} = E_{P_{XY}} \log \frac{P_{XY}}{P_X P_Y} \quad (1)$$

where  $P_X(x)$  and  $P_Y(y)$  present the marginal probability function of  $X$  and  $Y$  and  $P_{XY}$  presents the joint distribution function of  $X$  and  $Y$ , respectively.  $E_P$  is the expected value on the  $P$  distribution. For two continuous variables  $X$  and  $Y$  with a joint probability distribution of  $P_{XY}(x, y)$ , the value of MI of this distribution is denoted as  $I(X; Y)$  with the following formula:

$$I(X; Y) = \iint_y P_{XY}(x, y) \log \frac{P_{XY}(x, y)}{P_X(x)P_Y(y)} dx dy = E_{P_{XY}} \log \frac{P_{XY}}{P_X P_Y} \quad (2)$$

the formula for MI can be equivalent to the following:

$$\begin{aligned} I(X; Y) &= H(X) + H(Y) - H(X, Y) \\ &= H(X, Y) - H(Y) - H(Y|X) \end{aligned} \quad (3)$$

where  $H(X)$  and  $H(Y)$  are the boundary entropies.  $H(X|Y)$  and  $H(Y|X)$  are conditional entropies.  $H(X, Y)$  is the set of entropies of  $X$  and  $Y$ .

To fully grasp MI [22], we need to understand entropy and conditional entropy. According to Shannon, entropy quantifies uncertainty in a probability distribution. Uncertainty here means the “surprise” of the variable, which means the probability of a value in the variable is very low but it happens. Therefore, “surprise” will be inversely proportional to probability. Then, use the logarithm on the inverse of the

probability to return the values 0 and 1 to answer the question whether there is surprise in the event or not. If  $\frac{1}{p(x)}$  equals 1 leads to  $\log \log \left( \frac{1}{p(x)} \right)$  equals 0, this means there is no element of surprise in the event and is completely predictable. On the contrary,  $\frac{1}{p(x)}$  moving towards 0 leads to  $\log \log \left( \frac{1}{p(x)} \right)$ , then the result is indeterminate and “surprise” can occur because “surprise” is something that cannot be determined. Typically, in information systems, uncertainty is created in the information source (input) and transmission channel because we really do not know for sure which information source we receive and which signal is received [23]. In short, entropy (symbol:  $H(X)$ ) is a measure of the uncertainty of a random variable. The higher the entropy, the higher the uncertainty of a variable. Given a discrete and distributed random variable distributed according to  $P: X \rightarrow [0,1]$ , the formula for entropy is:

$$H(X) := \sum_{xx} P_X(x) \log \left( \frac{1}{P_X(x)} \right) = E[1 - \log \log(P_X(x))] \quad (4)$$

the formula for entropy with continuous variables is:

$$H(X) := - \int P_X(x) \log (P_X(x)) dx \quad (5)$$

from there, conditional entropy (symbol:  $H(Y|X)$ ) talks about the probability of variable  $X$  occurring without  $Y$ . Conditional entropy with discrete and continuous variables has the formula:

$$H(Y|X) = \sum_{xx,yy} P_{XY}(x,y) \log \frac{P_{XY}(x,y)}{P_X(x)} \quad (6)$$

$$H(Y|X) = \int P_{XY}(x,y) \log \frac{P_{XY}(x,y)}{P_X(x)} \quad (7)$$

Thus, we can rely on entropy to explain the MI algorithm as follows. If the probability of  $P_{XY}(x,y)$  approaching zero leads to a value  $\frac{P_{XY}(x,y)}{P_X(x)}$  of 0,  $(P_{XY}(x,y) \log \frac{P_{XY}(x,y)}{P_X(x)})$  will approach 0, which means that variable  $Y$  does not have much information related to  $X$ , then the value of MI is 0 and the two variables are completely independent. In case  $P_{XY}(x,y)$  it approaches one,  $\log \frac{P_{XY}(x,y)}{P_X(x)}$  it will gradually approach zero. This means that variable  $Y$  contains more information related to variable  $X$  and the less “surprise” happens between the two variables. Therefore, it can be concluded that the two variables are related or overlap (with  $\log \frac{P_{XY}(x,y)}{P_X(x)} = 0$  and  $P_{XY}(x,y) = 1$ ).

### 3. THE PROPOSED MODEL

The 3-stage architecture of the proposed model is shown in Figure 1. The shows as Figure 1 the process begins with data collection from flight data interface management unit and QAR systems, followed by decoding binary data and storing it in a structured data warehouse containing parametric data, technical documents, and knowledge models. Through preprocessing steps such as handling anomalies, reshaping data, and feature selection using mutual information, the study ensures that only relevant variables are used for model training. Two deep learning architectures, RNN and DNN, are implemented and fine-tuned to achieve optimal performance. The evaluation reveals that DNN outperforms RNN in terms of accuracy. After evaluation, parameters modification is applied for accuracy improvement.

This paper uses QAR data from an Airbus A320NEO [24]. Aircraft can record 600–3,000 parameters in a dataframe file, but due to computational, security, and storage constraints, only key parameters were selected including fuel flow, calibrated airspeed, static air temperature, pressure altitude, wind speed at the top of the cockpit, side wind speed, left landing gear, right landing gear, nose landing gear, standard acceleration [25]. The output is the fuel consumption rate, reflecting the fuel consumption flow. There are 9 input factors, removing redundant variables to optimize performance. After that, the dataset is split into 80% for training and 20% for testing. Based on a review of existing research, RNN and DNN are selected for comparison in next step. After building the model, training data is fed into the model to conduct learning. Aftermath, moving to model validation is check the reliability of the model. The test set data is fed into the models for learning and the estimated fuel consumption is obtained. Performance is assessed using mean squared error (MSE), root mean squared error (RMSE), R-squared ( $R^2$ ), and mean absolute error (MAE) to ensure reliability. The results are then compared with previous studies, and model weights are adjusted iteratively until optimal accuracy is achieved.

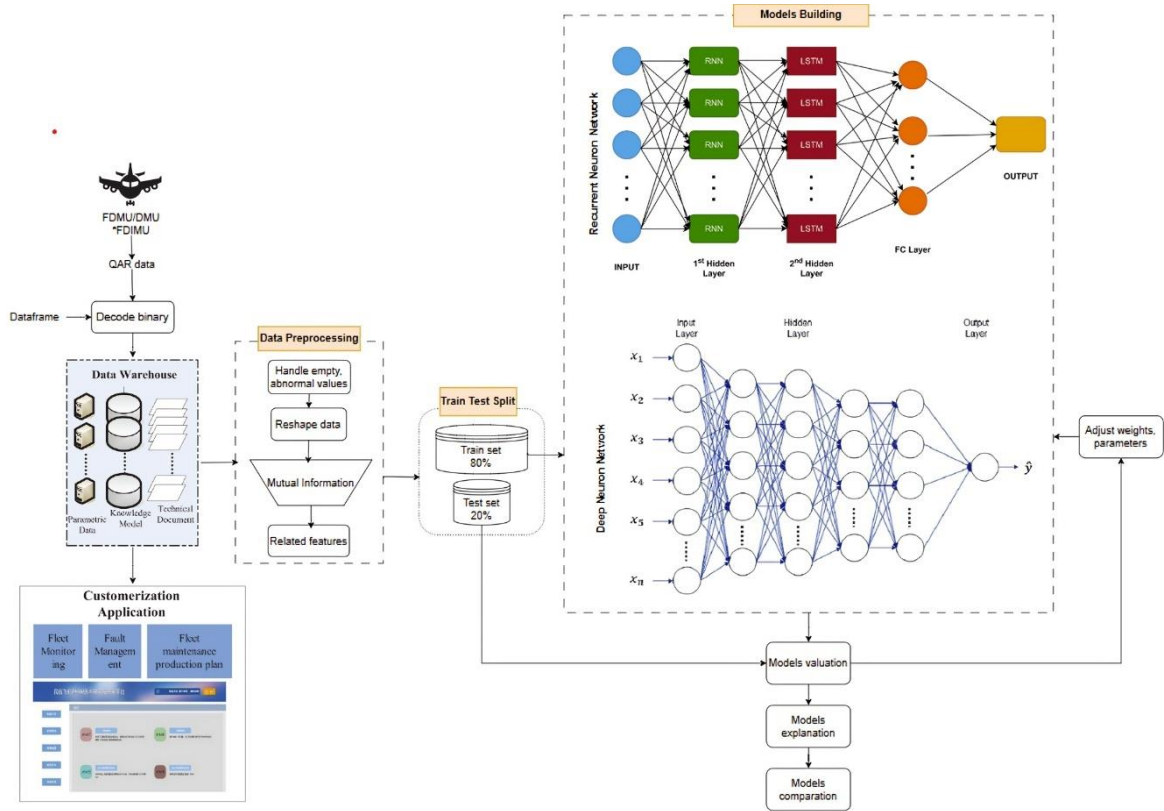


Figure 1. Architecture of proposed model

### 3.1. Data preprocessing

QAR is a digital recording device [26] that stores data in a binary format as a stream of bits, i.e., a sequence of 0 s and 1 s [27]. Storing data in binary format improves storage efficiency by reducing file size by up to ten times compared to formats such as CSV [28]. However, decoding binary data into meaningful technical values requires structured logic. This process adheres to the aeronautical radio incorporated (ARINC) standards, with ARINC 717 applied to older aircraft models and ARINC 767 used for newer ones [29]. A dataframe, a comprehensive text document, defines the structure, parameter locations, and decoding rules necessary for data interpretation [18]. The QAR continuously records data in 4-second blocks, with each second containing between 64 and 1024 words. Each subframe begins with a 12-bit synchronization word (e.g., 0x247, 0x5B8). A frame consists of four subframes, and the largest unit, the superframe, is determined by the frame counter (ranging from 0 to 4095). A new superframe begins whenever the frame counter modulo 16 equals zero (i.e., when  $\text{frame} \% 16 = 0$ ).

After decoding, the data is stored as a time series, including series ID, timestamp, and associated double and string values. The next step is to reshape the data to extract features by timestamp. In the cleaning step, the converted data is processed to handle outliers and missing values to ensure quality before splitting into training and testing sets.

### 3.2. Model training and validation

The data used for model estimation is historical data divided into a training set and an evaluation set. The data splitting is performed using stratified sampling based on the target variable labels, with a ratio of 80% for training and 20% for evaluation. The models are estimated using the Python libraries of TensorFlow. The model tuning parameters are described in the Table 1. This paper chooses four indicators to compare and evaluate, including MAE, MSE, RMSE, and  $R^2$  [30]:

- MAE is to measure accuracy for continuous variables [31]. The average absolute error has the following formula:

$$MAE = \frac{1}{n} \sum_{i=1}^n |e_i| \quad (8)$$

- The MSE is the risk function [32], corresponding to the expected value of the squared error loss.

$$MSE = \frac{1}{n} \sum_{i=1}^n (Y_i - \hat{Y}_i)^2 \quad (9)$$

- RMSE provides insight into the overall error distribution [33]. If they are equal, all errors have the same magnitude.

$$RMSE = \sqrt{\frac{1}{n} \sum_{i=1}^n e_i^2} \quad (10)$$

- $R^2$  provides information about the goodness of fit of a model [34]. The value of  $R^2$  will range from 0 to 1, where 1 indicates perfect prediction accuracy, while 0 means no correlation. A higher  $R^2$  signifies greater model reliability. The formula for this measure is as follows:

$$R^2 = 1 - \frac{\sum_{i=1}^n (Y_i - \hat{Y}_i)^2}{\sum_{i=1}^n (Y_i - \bar{Y})^2} \quad (11)$$

Table 1. Model tuning parameters in TensorFlow

Model	Layer	Decription in TensorFlow
RNN [35]	Embedding	Turns positive integers (indexes) into dense vectors of fixed size. The configured arguments are input_dim = 1.000, output_dim = 64.
	Long short-term memory (LSTM) [36]	Based on available runtime hardware and constraints, this layer will choose different implementations (cuDNN-based or backend-native) to maximize the performance. Unit is 128.
	Dense	Dense implements the operation: output = activation(dot(input, kernel) + bias) where activation is the element-wise activation function passed as the activation argument with 10 units.
DNN [37]	Dense	Dense implements the operation: output = activation(dot(input, kernel) + bias) where activation is the element-wise activation function passed as the activation argument (unit = 1)
	Dense	Dense implements the operation: output = activation(dot(input, kernel) + bias) where activation is the element-wise activation function passed as the activation argument named relu (configured arguments: unit = 64; activation = relu)
	Dense	Dense implements the operation: output = activation(dot(input, kernel) + bias) where activation is the element-wise activation function passed as the activation argument named relu (configured arguments: unit = 64; activation = relu)
	Dense	Dense implements the operation: output = activation(dot(input, kernel) + bias) where activation is the element-wise activation function passed as the activation argument (unit = 1)

### 3.3. Model selection and deployment

At this phase, a comprehensive evaluation of the model will be conducted, considering mention mesures: MAE, MSE, RMSE, and R squared ( $R^2$ ). A comparative analysis ensures the best-performing model maintains stability across training and test sets while optimizing key metrics. The selected model is then integrated with the MI method to establish a comprehensive selection process.

## 4. EXPERIMENTAL RESULTS

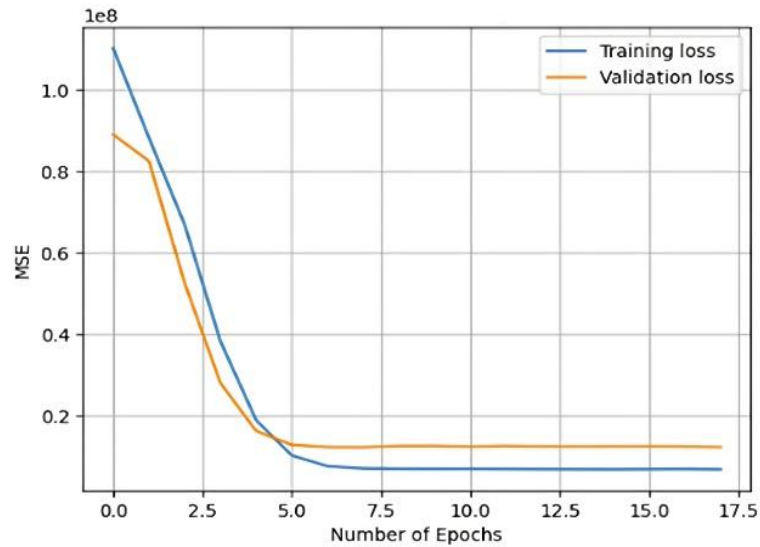
### 4.1. Model tuning and selection

Models are ranked based on performance metrics in the training set with trends analyzed on the evaluation set. The Figure 2(a) indicates a dcrease the loss function in both training and testing. DNN outperforms RNN with lower MAE (346.64 vs. 958.17) and RMSE (2811.2 vs. 3108.24), achieving 90% reliability ( $R^2 = 0.90$ ). However, due to overfitting tendencies, RNN is considered the more optimal model for fuel consumption prediction shown as Table 2.

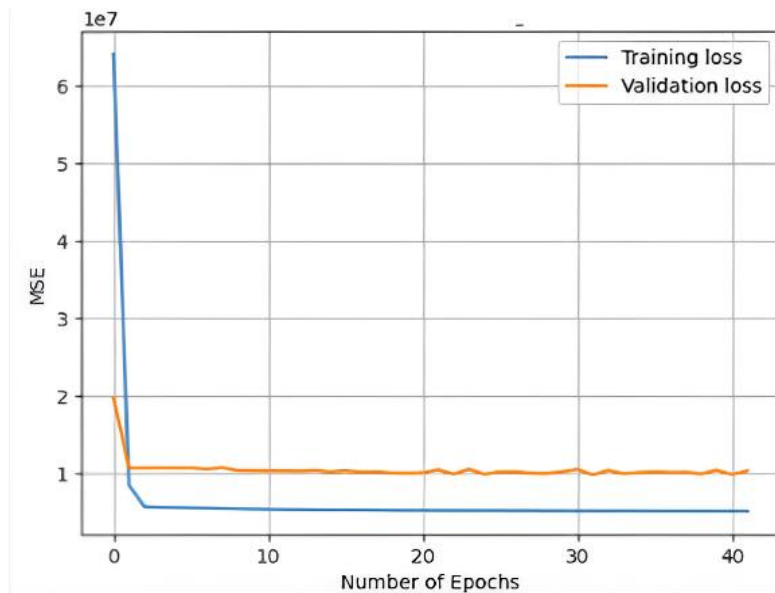
Besides, the model show no signs of underfitting or overfitting, with both training and evaluation loss functions decreasing. Convergence point at the 4<sup>th</sup> training time because no significant changes occur beyond this point (the 5<sup>th</sup> to 18<sup>th</sup> training times). Therefore, at the 4<sup>th</sup> training session the model is most effective. Similarly, Figure 2(b) show that the loss function in training and testing is decreasing. Besides, the model does not show signs of underfitting or overfitting.

Table 2. Indicators of two models RNN and DNN

Measuring indicators	MAE	MSE	RMSE	$R^2$
DNN	346.64	7902825.14	2811.2	0.90
RNN	958.17	9661184.19	3108.24	0.87



(a)



(b)

Figure 2. Evaluate model through MSE: (a) loss function in training and testing of RNN model and (b) loss function in training and testing of DNN model

At the same time, the model's loss function on training and evaluation set both decreased, reaching convergence point at the 2<sup>nd</sup> training time, with no significant changes from the 5<sup>th</sup> to 50<sup>th</sup> iteration. Therefore, at the second training session the model is most effective. However, the chart indicates slight underfitting, suggesting the need for additional parameters or a more complex model to prevent further underfitting.

The shown as Figures 3(a) and (b) compare the real value and predicted value, showing 87% accuracy for RNN and 90% for DNN, confirming DNN as the better model. Besides, the CNN model struggles with values in the 40,000–60,000 range, leading to errors. Meanwhile, the DNN model is forecasting with a lower error probability. Therefore, there are two directions to adjust this accuracy: (i) refining the model to better capture value fluctuations of aircraft and (ii) expanding the dataset, as the current study is based on a single flight. With the above accuracy, the models' accuracy aligns with [38] whose achieved each flight phase fluctuates around 90-99% accuracy; and 96% during takeoff.

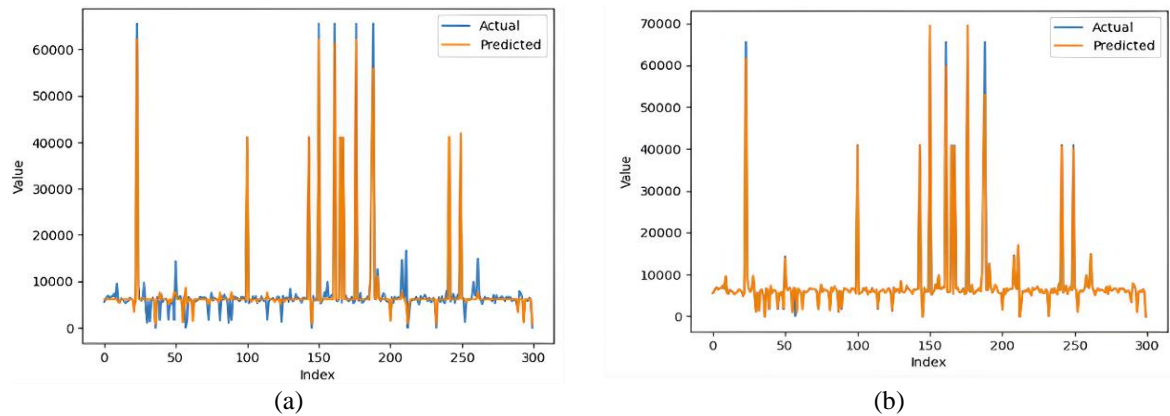


Figure 3. Evaluate model through actual vs predicted values: (a) prediction results of the RNN model and (b) prediction results of the DNN model

#### 4.2. Discussion

This study provides evidence that various factors such as calibrated airspeed, static air temperature, pressure altitude, wind speed at the cockpit, and side wind speed significantly impact civil aircraft fuel consumption. By leveraging two deep learning models DNN and RNN, the study highlights the effectiveness of parameter tuning to enhance prediction accuracy. Notably, the DNN model, when combined with the MI method for feature selection, achieved superior performance ( $R^2=90\%$ ,  $MAE=346.64$ ,  $MSE=7,902,825.14$ ), outperforming RNN. In comparison with [39]–[41], this research adopts a broader approach, considering multiple phases and integrating explicit feature selection. Additionally, the study emphasizes the advantage of deep learning over traditional statistical methods, showing that tuning model parameters significantly enhances prediction accuracy. Besides, earlier approaches often relied on traditional statistical methods or default configurations of machine learning algorithms, this study shows that parameter tuning can significantly improve predictive accuracy.

However, limitations exist, including reliance on specific environmental variables that may affect generalizability and the absence of real-time validation. The RNN model's lower performance suggests its temporal learning potential is not fully utilized. Future research should explore hybrid deep learning models (e.g., DNN with recurrent or transformer-based architectures) to capture both temporal and spatial dependencies. Transfer learning could further enhance adaptability across different aircraft types and flight conditions. To improve practical applicability, future work should focus on phase-specific modeling, real-time validation, multi-source data integration, and lightweight deep learning architectures to develop scalable and interpretable fuel consumption prediction models, optimizing aviation operations and reducing  $CO_2$  emissions.

#### 5. CONCLUSION

The findings of this study confirm that DNN with optimized parameter tuning and feature selection, outperform RNN in predicting aircraft fuel consumption. The combination of MI evaluation enhances automation, enabling faster forecasting and early detection of fuel anomalies, improving maintenance efficiency and cost-effectiveness. Despite its effectiveness, the model has several limitations that require improvement. The study is based on data from a single Airbus A320NEO flight, lacking validation across other Airbus and Boeing models, which differ in seating capacity, flight speed, and weight. It is necessary to expand and build more models for use with other aircraft models. Secondly, the dataset is limited, covering only one flight without distinguishing between takeoff, cruising, and landing phases, affecting prediction accuracy. The model has not been adjusted to predict each phase but is currently using a fixed model to predict the entire flight. Thirdly, the usage models are the foundation models for forecasting fuel consumption. Another challenge is handling abnormal values in QAR data, particularly in corrected airspeed and fuel flow, which distort predictions. While LSTM in RNN helps mitigate this, high error rates persist, necessitating more advanced techniques. Finally, the model relies solely on aircraft-recorded parameters, without incorporating external factors like weather and air traffic, limiting its adaptability to real-world conditions. To solve this problem, the model needs to research more external factors to calculate an acceptable index or value range to measure these factors in the model.



Research on MI variable selection method and deep learning models has led to an automated process for fuel prediction, opening new avenues for improvement. Specifically, there are two directions of development: depth and breadth. Developing in a broad direction, real-time anomaly detection can be built to alert airlines of potential risks and predict flight delays due to weather or operational factors. Aircraft to promptly take measures to prevent aviation accidents or potential and risky technical errors. In terms of depth, the model can be developed to incorporate additional variables beyond aircraft tracking data to enhance accuracy, minimize errors, and optimize fuel efficiency.

## ACKNOWLEDGMENTS

This research is funded by University of Economics Ho Chi Minh City, Vietnam (UEH)

## FUNDING INFORMATION

The authors declare that no external funding was received to support the research, data collection, analysis, or writing of this manuscript. This work was carried out independently without financial assistance from any public, commercial, or not-for-profit funding agency. Authors state no funding involved.

## AUTHOR CONTRIBUTIONS STATEMENT

This journal uses the Contributor Roles Taxonomy (CRediT) to recognize individual author contributions, reduce authorship disputes, and facilitate collaboration.

Name of Author	C	M	So	Va	Fo	I	R	D	O	E	Vi	Su	P	Fu
Quoc Hung Nguyen	✓	✓		✓	✓		✓			✓		✓	✓	✓
Hoang Lan Nguyen	✓	✓	✓		✓	✓	✓	✓	✓	✓	✓			

C : **C**onceptualization

M : **M**ethodology

So : **S**oftware

Va : **V**alidation

Fo : **F**ormal analysis

I : **I**nvestigation

R : **R**esources

D : **D**ata Curation

O : Writing - **O**riginal Draft

E : Writing - Review & **E**ding

Vi : **V**isualization

Su : **S**upervision

P : **P**roject administration

Fu : **F**unding acquisition

## CONFLICT OF INTEREST STATEMENT

The authors declare that they have no known competing financial interests or personal relationships that could have appeared to influence the work reported in this paper. Furthermore, the authors have no non-financial competing interests, such as political, ideological, academic, or intellectual conflicts, in relation to the content of this manuscript. Authors state no conflict of interest.

## INFORMED CONSENT

This paper does not involve any human participants, personal data, or identifiable information. Therefore, informed consent was not required. All data utilized in this research were derived from aircraft system recordings and technical sources that do not contain any private or sensitive information. The authors confirm that the study complies with ethical research standards and institutional guidelines.

## ETHICAL APPROVAL

This research did not involve any experiments on human participants or animals. Therefore, ethical review and approval were not applicable. All data used in this study were collected from aircraft systems and onboard sensors, which do not include personal, medical, or biological information. The authors affirm that the study was conducted in accordance with applicable institutional policies, ethical research principles, and national regulations concerning non-human-subject research. No ethical violations occurred during the course of this paper.



## DATA AVAILABILITY

The Quick Access Recorder (QAR) flight-data used in this study were obtained under a confidentiality agreement with the partner airline and contain commercially sensitive operational information. Therefore, the raw QAR files cannot be shared publicly.

Processed feature tables, model-training scripts, and a de-identified synthetic sample sufficient to reproduce the reported results are available from the corresponding author, Quoc Hung Nguyen (hungnq@ueh.edu.vn), upon reasonable request for non-commercial research purposes and subject to a signed non-disclosure agreement.





## REFERENCES

- [1] J. Yanto and R. P. Liem, "Aircraft fuel burn performance study: A data-enhanced modeling approach," *Transportation Research Part D: Transport and Environment*, vol. 65, pp. 574–595, Dec. 2018, doi: 10.1016/j.trd.2018.09.014.
- [2] D. S. Lee *et al.*, "Aviation and global climate change in the 21st century," *Atmospheric Environment*, vol. 43, no. 22–23, pp. 3520–3537, Jul. 2009, doi: 10.1016/j.atmosenv.2009.04.024.
- [3] K. s. Yin, P. Dargusch, and A. Halog, "An analysis of the greenhouse gas emissions profile of airlines flying the Australian international market," *Journal of Air Transport Management*, vol. 47, pp. 218–229, Aug. 2015, doi: 10.1016/j.jairtraman.2015.06.005.
- [4] J. M. Collins and D. McLarty, "All-electric commercial aviation with solid oxide fuel cell-gas turbine-battery hybrids," *Applied Energy*, vol. 265, p. 114787, May 2020, doi: 10.1016/j.apenergy.2020.114787.
- [5] J. K. Brueckner and C. Abreu, "Airline fuel usage and carbon emissions: Determining factors," *Journal of Air Transport Management*, vol. 62, pp. 10–17, Jul. 2017, doi: 10.1016/j.jairtraman.2017.01.004.
- [6] S. Ekici, M. Ayar, U. Kilic, and T. H. Karakoc, "Performance based analysis for the Ankara-London route in terms of emissions and fuel consumption of different combinations of aircraft/engine: An IMPACT application," *Journal of Air Transport Management*, vol. 108, p. 102357, May 2023, doi: 10.1016/j.jairtraman.2022.102357.
- [7] S. Gössling and J. Higham, "The Low-Carbon Imperative: Destination Management under Urgent Climate Change," *Journal of Travel Research*, vol. 60, no. 6, pp. 1167–1179, Jul. 2021, doi: 10.1177/0047287520933679.
- [8] S. Becken and B. Mackey, "What role for offsetting aviation greenhouse gas emissions in a deep-cut carbon world?," *Journal of Air Transport Management*, vol. 63, pp. 71–83, Aug. 2017, doi: 10.1016/j.jairtraman.2017.05.009.
- [9] C. A. Arter, J. J. Buonocore, C. Moniruzzaman, D. Yang, J. Huang, and S. Arunachalam, "Air quality and health-related impacts of traditional and alternate jet fuels from airport aircraft operations in the U.S.," *Environment International*, vol. 158, p. 106958, Jan. 2022, doi: 10.1016/j.envint.2021.106958.
- [10] M. Grote, I. Williams, and J. Preston, "Direct carbon dioxide emissions from civil aircraft," *Atmospheric Environment*, vol. 95, pp. 214–224, Oct. 2014, doi: 10.1016/j.atmosenv.2014.06.042.
- [11] G. P. Brasseur *et al.*, "Impact of aviation on climate: FAA's Aviation Climate Change Research Initiative (ACCRI) phase II," *Bulletin of the American Meteorological Society*, vol. 97, no. 4, pp. 561–583, Apr. 2016, doi: 10.1175/BAMS-D-13-00089.1.
- [12] S. Ekici, M. Ayar, I. Orhan, and T. H. Karakoc, "Cruise altitude patterns for minimizing fuel consumption and emission: A detailed analysis of five prominent aircraft," *Energy*, vol. 295, p. 130989, May 2024, doi: 10.1016/j.energy.2024.130989.
- [13] D. S. Lee *et al.*, "Transport impacts on atmosphere and climate: Aviation," *Atmospheric Environment*, vol. 44, no. 37, pp. 4678–4734, Dec. 2010, doi: 10.1016/j.atmosenv.2009.06.005.
- [14] Y. Hui and M. Fanxing, "Application of Improved SAX Algorithm to QAR Flight Data," *Physics Procedia*, vol. 24, pp. 1406–1413, 2012, doi: 10.1016/j.phpro.2012.02.209.
- [15] L. Wang, C. Wu, and R. Sun, "An analysis of flight Quick Access Recorder (QAR) data and its applications in preventing landing incidents," *Reliability Engineering and System Safety*, vol. 127, pp. 86–96, Jul. 2014, doi: 10.1016/j.res.2014.03.013.
- [16] W. H. Pan, Y. W. Feng, C. Lu, and J. Q. Liu, "Analyzing the operation reliability of aeroengine using Quick Access Recorder flight data," *Reliability Engineering and System Safety*, vol. 235, p. 109193, Jul. 2023, doi: 10.1016/j.res.2023.109193.
- [17] M. Strohmeier, V. Lenders, and I. Martinovic, "On the security of the automatic dependent surveillance-broadcast protocol," *IEEE Communications Surveys and Tutorials*, vol. 17, no. 2, pp. 1066–1087, 2015, doi: 10.1109/COMST.2014.2365951.
- [18] A. Grebenssek and T. Magister, "Effect of seasonal traffic variability on the performance of air navigation service providers," *Journal of Air Transport Management*, vol. 25, pp. 22–25, Dec. 2012, doi: 10.1016/j.jairtraman.2012.04.003.
- [19] J. He, L. Qu, P. Wang, and Z. Li, "An oscillatory particle swarm optimization feature selection algorithm for hybrid data based on mutual information entropy," *Applied Soft Computing*, vol. 152, p. 111261, Feb. 2024, doi: 10.1016/j.asoc.2024.111261.
- [20] B. K. Burian, K. L. Mosier, U. M. Fischer, and J. A. Kochan, "New teams on the flight deck: Humans and context-sensitive information automation," in *Human Factors in Aviation and Aerospace, Third Edition*, Elsevier, 2022, pp. 59–87, doi: 10.1016/B978-0-12-420139-2.00008-3.
- [21] P. Latham and Y. Roudi, "Mutual information," *Scholarpedia*, vol. 4, no. 1, p. 1658, 2009, doi: 10.4249/scholarpedia.1658.
- [22] C. Hu, J. Wu, C. Sun, X. Chen, and R. Yan, "Mutual information-based feature disentangled network for anomaly detection under variable working conditions," *Mechanical Systems and Signal Processing*, vol. 204, p. 110804, Dec. 2023, doi: 10.1016/j.ymssp.2023.110804.
- [23] J. Mensah, "Sustainable development: Meaning, history, principles, pillars, and implications for human action: Literature review," *Cogent Social Sciences*, vol. 5, no. 1, Jan. 2019, doi: 10.1080/233111886.2019.1653531.
- [24] S. Ekici, "Thermodynamic mapping of A321-200 in terms of performance parameters, sustainability indicators and thermo-ecological performance at various flight phases," *Energy*, vol. 202, p. 117692, Jul. 2020, doi: 10.1016/j.energy.2020.117692.
- [25] C. Tong, X. Yin, S. Wang, and Z. Zheng, "A novel deep learning method for aircraft landing speed prediction based on cloud-based sensor data," *Future Generation Computer Systems*, vol. 88, pp. 552–558, Nov. 2018, doi: 10.1016/j.future.2018.06.023.
- [26] C. E. Lan, K. Wu, and J. Yu, "Flight characteristics analysis based on QAR data of a jet transport during landing at a high-altitude airport," *Chinese Journal of Aeronautics*, vol. 25, no. 1, pp. 13–24, Feb. 2012, doi: 10.1016/S1000-9361(11)60357-9.
- [27] G. Walker, "Electronic Data Recorders," in *Encyclopedia of Forensic Sciences: Volume 1-4, Third Edition*, Elsevier, 2022, pp. 237–248, doi: 10.1016/B978-0-12-823677-2.00144-6.
- [28] F. Schwaiger and F. Holzapfel, "Fast decoding of arinc 717 flight data recordings," in *AIAA Scitech 2021 Forum*, Reston, Virginia: American Institute of Aeronautics and Astronautics, Jan. 2021, pp. 1–12, doi: 10.2514/6.2021-1982.


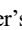
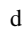

- [29] J. J. Rowland and M. Lawton, "A versatile microprocessor-based synchronization decoder for replay from flight data recorders," *Journal of Microcomputer Applications*, vol. 12, no. 1, pp. 87–93, Jan. 1989, doi: 10.1016/0745-7138(89)90009-2.
- [30] M. Steurer, R. J. Hill, and N. Pfeifer, "Metrics for evaluating the performance of machine learning based automated valuation models," *Journal of Property Research*, vol. 38, no. 2, pp. 99–129, Apr. 2021, doi: 10.1080/09599916.2020.1858937.
- [31] C. J. Willmott and K. Matsuura, "Advantages of the mean absolute error (MAE) over the root mean square error (RMSE) in assessing average model performance," *Climate Research*, vol. 30, no. 1, pp. 79–82, 2005, doi: 10.3354/cr030079.
- [32] T. Hastie, J. Friedman, and R. Tibshirani, *The Elements of Statistical Learning*. in Springer Series in Statistics. New York, NY: Springer New York, 2001, doi: 10.1007/978-0-387-21606-5.
- [33] T. Chai and R. R. Draxler, "Root Mean Square Error (RMSE) or Mean Absolute Error (MAE)," *Geoscientific Model Development*, vol. 7, pp. 1525–1534, 2014.
- [34] C. L. Cheng, Shalabh, and G. Garg, "Coefficient of determination for multiple measurement error models," *Journal of Multivariate Analysis*, vol. 126, pp. 137–152, Apr. 2014, doi: 10.1016/j.jmva.2014.01.006.
- [35] C. Fu *et al.*, "Prediction of emission characteristics of diesel/n-hexanol/graphene oxide blended fuels based on fast outlier detection-sparrow search algorithm-bidirectional recurrent neural network," *Process Safety and Environmental Protection*, vol. 187, pp. 1076–1096, Jul. 2024, doi: 10.1016/j.psep.2024.05.027.
- [36] J. Zhang and S. Li, "Air quality index forecast in Beijing based on CNN-LSTM multi-model," *Chemosphere*, vol. 308, p. 136180, Dec. 2022, doi: 10.1016/j.chemosphere.2022.136180.
- [37] G. E. Hinton, S. Osindero, and Y. W. Teh, "A fast learning algorithm for deep belief nets," *Neural Computation*, vol. 18, no. 7, pp. 1527–1554, Jul. 2006, doi: 10.1162/neco.2006.18.7.1527.
- [38] T. Baklacioglu, "Modeling the fuel flow-rate of transport aircraft during flight phases using genetic algorithm-optimized neural networks," *Aerospace Science and Technology*, vol. 49, pp. 52–62, Feb. 2016, doi: 10.1016/j.ast.2015.11.031.
- [39] M. Zhang, Q. Huang, S. Liu, and Y. Zhang, "Fuel consumption model of the climbing phase of departure aircraft based on flight data analysis," *Sustainability (Switzerland)*, vol. 11, no. 16, p. 4362, Aug. 2019, doi: 10.3390/su11164362.
- [40] S. Atipan and P. Chomdej, "Fuel Consumption Analysis of Gradual Climb Procedure with Varied Climb Angle and Airspeed," *Sustainable Aviation. Springer International Publishing*, 2023, pp. 315–320, doi: 10.1007/978-3-031-37943-7\_42.
- [41] L. Zhang, A. Bian, C. Jiang, and L. Wu, "A Comprehensive Framework for Estimating Aircraft Fuel Consumption Based on Flight Trajectories," *arXiv*, Sep. 2024, doi: 10.48550/arXiv.2409.05429.

## BIOGRAPHIES OF AUTHORS



**Quoc Hung Nguyen**     is a senior lecturer and researcher at the School of Business Information Technology, UEH College of Technology and Design, University of Economics Ho Chi Minh City (UEH), Vietnam. He received his Ph.D. in Computer Science from Hanoi University of Science and Technology (HUST) in 2016. His research interests include big data analytics methods using artificial intelligence and blockchain encryption technology, with applications in the fields of economics, business, science, technology, medicine, agriculture, and more. He can be contacted at email: hungngq@ueh.edu.vn.



**Hoang Lan Nguyen**     is a Master's degree holder in Information Design and Technology from the University of Economics Ho Chi Minh City. Currently, she holds the position of Data Engineer at FPT Software in Vietnam. She can be contacted at email: lannguyen.212118005@st.ueh.edu.vn.